

Efficient and Accurate MTF Measurement for Spatially Non-uniform Paper

Masayuki Ukishima, Norimichi Tsumura and Toshiya Nakaguchi
Graduate Course of Advanced Integration Science, Chiba University, Japan
ukishima@graduate.chiba-u.jp

Markku Hauta-Kasari and Jussi Parkkinen
Department of Computer Science, University of Joensuu, Finland

Yoichi Miyake
Research Center for Frontier Medical Engineering, Chiba University, Japan

Abstract

The conventional Koopipat's method was modified to measure the modulation transfer function (MTF) of spatially non-uniform paper. First, we analyzed and removed the non-uniform characteristic caused by the fiber structure of paper. Secondly, in order to calculate the paper MTF, the edge spread function (ESF) was analyzed using the edge part of a neutral density (ND) filter superposed on paper. A microscope which can illuminate paper from front or back side was used to measure the ESF. Gans' method was used to calculate the Fourier transform of ESF. MTFs were measured for three types of paper: uncoated paper, coated paper and glossy paper, whose graininess levels are high, normal and low, respectively. As a result of the experiment, regardless of graininess level, the MTFs were measured efficiently and accurately. The measured MTF was applied to predict reflectance distribution of monochrome inkjet images from transmittance distribution. We conclude that our method is effective to simulate inkjet printing since the RMSE and difference of average reflectance between the measured and predicted data were low.

Introduction

Printed images on paper are widely used for magazines, books, posters and so on. Image quality of these images is significantly influenced by optical characteristics of paper. Paper is a well-known turbid medium, and incident light into paper is scattered in paper. This phenomenon causes optical dot gain which influences on image quality such as tone reproduction, color reproduction, sharpness and graininess of halftone print images. Therefore, it is necessary to quantify the light scattering characteristic of paper to evaluate the image quality of printed images.

The light scattering phenomenon can be represented by the point spread function (PSF) of paper. The Fourier transform of the PSF is defined as the modulation transfer function (MTF). If the paper MTF is obtained, the PSF can be calculated by inverse Fourier transform. Inoue et al. measured the paper MTF by projecting sinusoidal test patterns to paper and scanning the modulation with a micro-densitometer [1]. They also proposed the reflection image model, and applied the measured MTF to evaluate image quality of halftone images based on the reflection image model [2]. Though their measurement method of MTF has high accuracy, it needs a lot of measurement time and special instru-

ments. Then, Koopipat et al. proposed more efficient method [3]. They measured the paper MTF by capturing the paper superposed an optically knife-edge chart with a microscope and analyzing the captured image based on the reflection image model. Their method is efficient since the measurement time is short. However, the measured MTF was noisy, particularly for paper having spatially non-uniform characteristic.

In this paper, we modify the conventional Koopipat's method to measure the MTF of spatially non-uniform paper with a high degree of accuracy without losing its efficiency. The MTFs are measured for three types of paper such as uncoated, coated and glossy paper. The uncoated paper has a great non-uniform characteristic and it is difficult to measure its MTF accurately by the original Koopipat's method. The measured MTF of glossy paper is applied to predict reflectance distribution of inkjet images based on the reflection image model.

Conventional Method for Measuring Paper MTF Based on Reflection and Transparency Image Model

Koopipat et al. proposed a method [3] to measure the paper MTF based on the reflection and transparency image models illustrated as Fig. 1. The reflection image model predicts the reflectance of halftone images [2] and is defined as

$$r(x, y) = \{t_i(x, y) * \text{PSF}_p(x, y)\} r_p t_i(x, y), \quad (1)$$

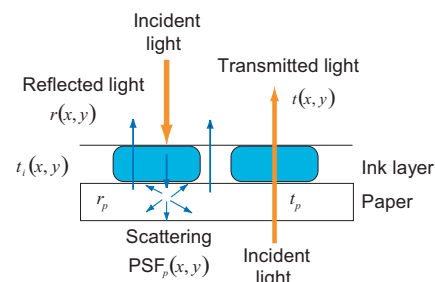


Figure 1. The reflection and transparency image models.

where (x, y) denotes spatial coordinates, $r(x, y)$ is reflectance of the halftone image, $t_i(x, y)$ is transmittance of the ink layer, $\text{PSF}_p(x, y)$ is the point spread function of paper, r_p is reflectance of paper and $*$ denotes convolution operation. The transparency image model predicts the transmittance of halftone images and is defined as

$$t(x, y) = t_p t_i(x, y), \quad (2)$$

where $t(x, y)$ is transmittance of the halftone image and t_p is transmittance of paper. By substituting $t_i(x, y)$ of Eq. (2) to Eq. (1), we can obtain

$$\frac{r(x, y)}{r_p} / \frac{t(x, y)}{t_p} = \frac{t(x, y)}{t_p} * \text{PSF}_p(x, y). \quad (3)$$

The paper MTF can be obtained from the Fourier transform of Eq. (3):

$$\text{MTF}_p(u, v) = \mathcal{F} \left\{ \frac{r(x, y)}{r_p} / \frac{t(x, y)}{t_p} \right\} / \mathcal{F} \left\{ \frac{t(x, y)}{t_p} \right\}, \quad (4)$$

where (u, v) denotes coordinates of spatial frequency, $\text{MTF}_p(u, v)$ is the paper MTF and $\mathcal{F}\{f(x)\}$ denotes the Fourier transform of $f(x)$.

In the measurement by Koopipat et al., a knife-edge chart (a sharp-edge image on the glass) was set on the paper as the virtual ink layer, and reflectance $r(x, y)$ and transmittance $t(x, y)$ are measured with an optical microscope which can illuminate paper from front or back side of the paper. The obtained two-dimensional edge images, $r(x, y)$ and $t(x, y)$, were converted into the one-dimensional functions, $r(x)$ and $t(x)$, by calculating average of these images in the direction of y which is parallel to edge. Since $r(x)$ and $t(x)$ are edge spread function (ESF) in this case, the paper MTF is obtained from the Fourier transform of Eq. (3) after derivation operation:

$$\text{MTF}_p(u) = k \cdot \mathcal{F} \left\{ \frac{d}{dx} \frac{r(x)}{t(x)} \right\} / \mathcal{F} \left\{ \frac{d}{dx} t(x) \right\}, \quad (5)$$

where

$$k = t_p^2 / r_p. \quad (6)$$

The constant value k can be decided to be $\text{MTF}_p(0) = 1$. The merit of this method is that only two images, $r(x, y)$ and $t(x, y)$, are required to obtain the paper MTF, and the instrument setting is simple. However, the obtained MTF curve is not smooth [Ref. 3, Fig. 6], especially for the uncoted paper. This is because the graininess of the uncoted paper is high due to the fiber structure of paper, and the obtained MTF curve contains the spatial frequency component of the fiber structure. Furthermore, the derivation in Eq. (5) amplifies the spatial frequency component of the fiber structure. In order to obtain the MTF curve smoothly, it is necessary to remove this noise due to the fiber structure.

Proposed Method

Revised Reflection and Transparency Image Model

In the reflection and transparency image models, reflectance r_p and transmittance t_p of paper are assumed to be constant. These assumptions are valid in macroscopic view. In microscopic view, however, most of paper has spatially non-uniform characteristic because of the fiber structure as shown in Fig. 4(b)(e), Fig.

5(b)(e) and Fig. 6(b)(e). To solve this problem, we revised r_p and t_p to functions of spatial coordinates, $r_p(x, y)$ and $t_p(x, y)$. Then, Eq. (4) is converted as

$$\text{MTF}_p(u, v) = \mathcal{F} \left\{ \frac{r(x, y)}{r_p(x, y)} / \frac{t(x, y)}{t_p(x, y)} \right\} / \mathcal{F} \left\{ \frac{t(x, y)}{t_p(x, y)} \right\}. \quad (7)$$

Equation (7) has two fractional factors, $r(x, y) / r_p(x, y)$ and $t(x, y) / t_p(x, y)$. The function $r(x, y)$ and $r_p(x, y)$ have the same fiber structure. The function $t(x, y)$ and $t_p(x, y)$ also have the same fiber structure. Therefore, these division operations are able to cancel the spatial non-uniformity of paper.

Adopting Gans' Method for Fourier Transform of Edge Spread Function

Without differential operation, the Fourier transform of edge function can be calculated using Gans' method [4, 5, 6]. In Gans' method, a rectangular function $f_r(x)$ is obtained by the following formula in order to calculate the Fourier transform of an edge function $f_i(x)$.

$$f_r(x) = f_i(x) - f_i(x - a), \quad (8)$$

where $f_i(x - a)$ is the edge function which is obtained by shifting $f_i(x)$ in arbitrary length of a . The Fourier transform of $f_r(x)$ is given by

$$\begin{aligned} F_r(u) &= \int_{-\infty}^{\infty} f_r(x) e^{-jux} dx \\ &= \int_{-\infty}^{\infty} \{f_i(x) - f_i(x - a)\} e^{-jux} dx \\ &= F_i(u) [1 - e^{-jua}], \end{aligned} \quad (9)$$

$$\therefore F_i(u) = \frac{F_r(u)}{1 - e^{-jua}}, \quad (10)$$

where $F_r(u)$ and $F_i(u)$ are Fourier transform of $f_r(x)$ and $f_i(x)$, respectively. Gans' method is somewhat more inefficient than usage of derivation since $f_i(x - a)$ is needed to measure as well as $f_i(x)$. However, we adopted Gans' method since the difference of efficiency is a little, and the accuracy of calculation of this method is better than that of derivation operation.

Measurement Experiment of Paper MTF Samples and Instruments

Using our proposed method described in the previous section, we measured the MTFs of three types of paper: uncoated paper, coated paper and glossy paper, whose graininess levels are high, normal and low, respectively (Fig. 4(b)(e), Fig. 5(b)(e) and Fig. 6(b)(e)).

In the experiment by Koopipat et al., they used a knife-edge chart as the virtual ink layer. However, we consider that kind of chart should not be used. The transmittance $t_c(x, y)$ of a knife-edge chart is generally as

$$t_c(x, y) = \begin{cases} 0 & x \leq x_1 \\ 1 & x > x_1 \end{cases}, \quad (11)$$

where x_1 is the step part of the edge. The transmittance $t_c(x, y)$ corresponds to $t_i(x, y)$ in Eq. (3). Equation (11) means that Eq. (3) can not be defined at $x \leq x_1$ since $t_i(x, y)$ is invariably zero. We have to analyze the only data at $x > x_1$. To solve this problem, we used a neutral density (ND) filter whose optical density is 0.8

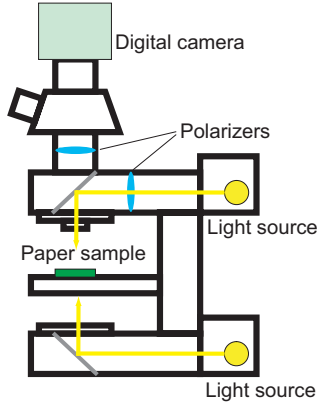


Figure 2. Optical microscope for reflectance and transmittance measurement.

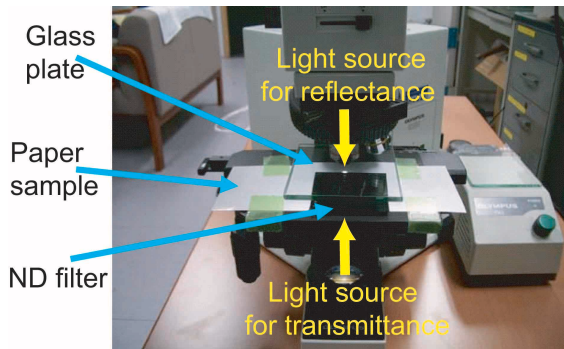


Figure 3. Measurement system. A glass plate is superposed on the sample to contact closely the paper and ND filter.

as the virtual ink layer instead of the knife-edge chart. The optical density 0.8 was selected empirically so that measured values fall into the dynamic range of the camera.

The measurement was performed with an optical microscope which can illuminate paper from front or back side of the paper like Koopipat's experiment (Fig. 2). A monochrome digital camera (INFINITY4-11M, Lumenera corp., CCD, USB2.0) was attached to the microscope. The maximum resolution of this camera is 4008x2672. The center area (1400x400) was used for the analysis. The pixel pitch of the CCD sensor in this camera is about $2.2\mu\text{m}$ when the magnification of the optical system is $4\times$. To convert the light source to white color, two daylight-balanced (LBD) filters were placed in front of each light source. To eliminate the specular reflection component, two polarizers were placed in front of the light source for reflection and of the camera, respectively.

Measurement of Paper MTF

Figure 3 shows our measurement system. The measurement was performed as a following procedure.

1. Images $r(x,y)$ and $t(x,y)$ were obtained by capturing the edge part of ND filter superposed on paper (the virtual print image) using the microscope with each light source for reflection and transmission, respectively.
2. After removing the ND filter, paper images $r_p(x,y)$ and $t_p(x,y)$ were obtained using the microscope, respectively.

3. After superposing the ND filter again and shifting the virtual print image in length of a for the horizontal direction, images $r(x-a,y)$ and $t(x-a,y)$ were obtained using the microscope, respectively.
4. After removing the ND filter again, paper images $r_p(x-a,y)$ and $t_p(x-a,y)$ were obtained using the microscope, respectively.
5. The fiber structure was cancelled by following operations.

$$r_i(x,y) = \frac{r(x,y)}{r_p(x,y)}, \quad (12)$$

$$t_i(x,y) = \frac{t(x,y)}{t_p(x,y)}, \quad (13)$$

$$r_i(x-a,y) = \frac{r(x-a,y)}{r_p(x-a,y)}, \quad (14)$$

$$t_i(x-a,y) = \frac{t(x-a,y)}{t_p(x-a,y)}. \quad (15)$$

6. Four edge spread functions were obtained by calculating averages of $r_i(x,y)$, $t_i(x,y)$, $r_i(x-a,y)$ and $t_i(x-a,y)$:

$$r_i(x) = \frac{1}{l_y} \int_0^{l_y} r_i(x,y) dy, \quad (16)$$

$$t_i(x) = \frac{1}{l_y} \int_0^{l_y} t_i(x,y) dy, \quad (17)$$

$$r_i(x-a) = \frac{1}{l_y} \int_0^{l_y} r_i(x-a,y) dy, \quad (18)$$

$$t_i(x-a) = \frac{1}{l_y} \int_0^{l_y} t_i(x-a,y) dy, \quad (19)$$

where l_y is height of captured images.

7. Each transmittance $t_i(x)$ and $t_i(x-a)$ was compensated (described in detail in the next Subsection).
8. The Fourier transform $\mathfrak{F}\{t_i(x)\}$ was calculated by Gans' method using $t_i(x)$ and $t_i(x-a)$ based on Eqs. (8), (9) and (10).
9. The Fourier transform $\mathfrak{F}\{r_i(x)/t_i(x)\}$ was also calculated by Gans' method using $r_i(x)/t_i(x)$ and $r_i(x-a)/t_i(x-a)$ based on Eqs. (8), (9) and (10).
10. Based on Eq. (7), the paper MTF was calculated as

$$\text{MTF}_p(u) = \mathfrak{F}\left\{\frac{r_i(x)}{t_i(x)}\right\} / \mathfrak{F}\{t_i(x)\}. \quad (20)$$

The obtained images, $r(x,y)$, $r_p(x,y)$, $r_i(x,y)$, $t(x,y)$, $t_p(x,y)$ and $t_i(x,y)$, of each type of paper are shown in Figs. 4, 5 and 6.

Compensation of Ink Transmittance

Based on Eqs. (3), (12), and (13), if the transmittance of ink layer $t_i(x,y)$ is constant value, the paper PSF can be ignored, and it is theoretically derived that

$$t_i = \sqrt{r_i}. \quad (21)$$

In practice, however, t_i is observed lower than $\sqrt{r_i}$ when the density of t_i is high, particularly. It is considered this phenomenon

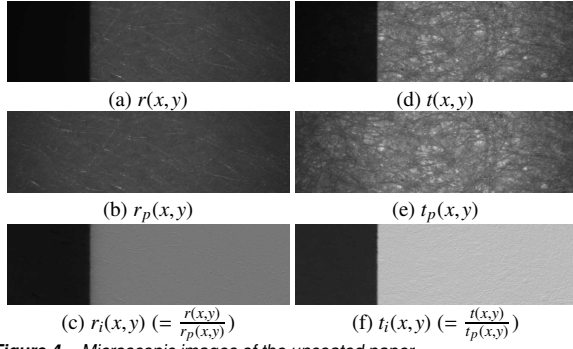


Figure 4. Microscopic images of the uncoated paper.

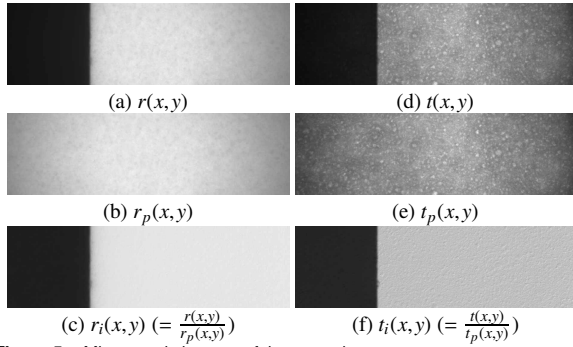


Figure 5. Microscopic images of the coated paper.

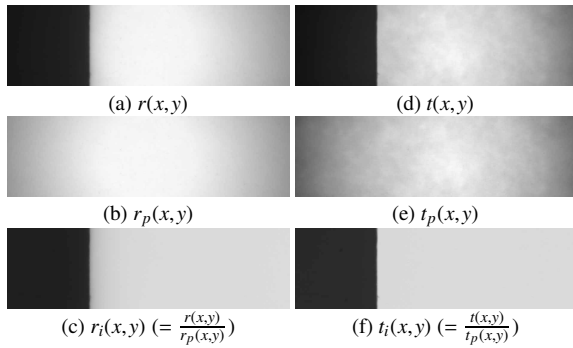


Figure 6. Microscopic images of the glossy paper.

is caused by the carrier coefficient, specular reflection, multiple reflections between the ink layer and paper layer, and so on. This phenomenon leads to serious error when $r_i(x)/t_i(x)$ and $r_i(x-a)/t_i(x-a)$ are calculated in the process 9 described in the previous Subsection. To solve this problem, we analyzed the relationships between t_i and $\sqrt{r_i}$ for several optical densities, and compensated $t_i(x)$ and $t_i(x-a)$ as a following procedure.

1. Using the microscope, we measured t_i and $\sqrt{r_i}$ of the paper superposed ND filters whose optical density are 0.2, 0.4, 0.6, 0.8 or 1.0, respectively. The example of this result for the glossy paper is shown in Fig. 7. The solid line is the fitting curve given by

$$\sqrt{r_i} = b(t_i)^c + (1-b), \quad (22)$$

where b and c are fitting coefficients.

2. The real $t_i(x)$ and $t_i(x-a)$ measured in the process 6 described in the previous Subsection were substituted into t_i

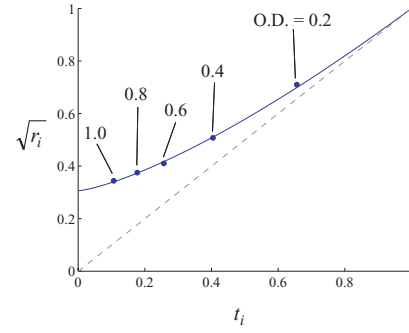


Figure 7. The relationships between t_i and $\sqrt{r_i}$. In this graph, O.D. denotes the optical density of ND filter.

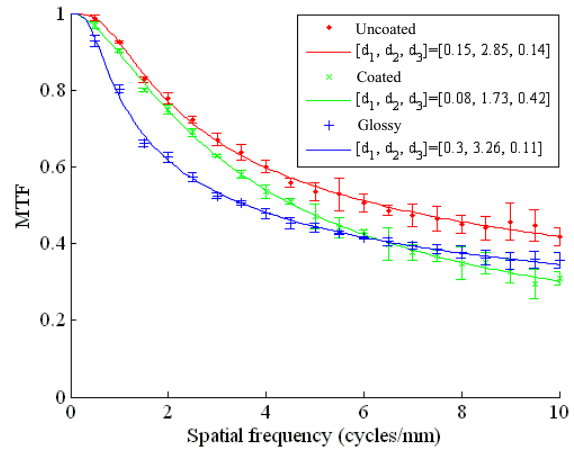


Figure 8. Measured paper MTFs.

of left-hand side of Eq. (22) for each x , and compensated $t_i(x)$ and $t_i(x-a)$ were calculated.

The compensated $t_i(x)$ and $t_i(x-a)$ satisfy Eq. (21). This procedure correspond to the process 7 described in the previous Subsection.

Results and Discussions

Figure 8 shows the measured MTF of each type of paper. Each paper MTF curve was smooth and noiseless significantly regardless of graininess level of paper. We measured the MTF three times at different positions for each type of paper, and error bars are plotted. Since the error bars were short, we consider the proposed method is stable. The solid lines are the fitting curves of the measured data given by

$$\text{MTF}(u) = \frac{1}{[1 + (2\pi d_1 u)^{d_2}]^{d_3}}, \quad (23)$$

where d_1 , d_2 and d_3 are fitting coefficients.

Figure 9 shows comparison of the uncoated paper MTFs calculated by derivation or by Gans' method. In case of using derivation, the MTF were calculated by

$$\text{MTF}_P(u) = \mathfrak{F} \left\{ \frac{d}{dx} \frac{r_i(x)}{t_i(x)} \right\} / \mathfrak{F} \left\{ \frac{d}{dx} t_i(x) \right\}. \quad (24)$$

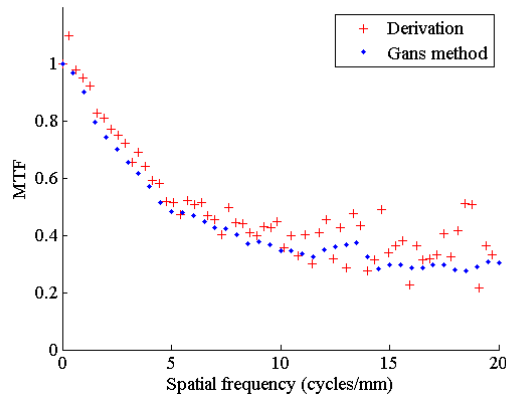


Figure 9. Comparison of the uncoated paper MTFs calculated by derivation and by Gans' method.

If we use derivation, the measured paper MTF is relatively smooth since we cancelled the fiber structure of paper by the process 5 described in the previous Subsection. However, the use of Gans' method is more effective than that of derivation.

Predicting Reflectance Distribution of Inkjet Image

The MTFs of uncoated paper, coated paper and glossy paper were measured in the previous section. In this section, we simulate reflectance distribution of inkjet halftone images printed on glossy paper from transmittance distribution using the glossy paper MTF based on the reflection and transparency image models. A special inkjet printer for medical X-ray images (CXJ3000, CANON) was used to print. This printer can jet five types of monochrome inks of different optical density. The resolution is 1200 dots per inch. The 12bit tone can be reproduced. The predicting simulation was performed using unity type of ink of the most dense one or five types of ink, respectively as a following procedure.

1. The PSF of glossy paper, $PSF_p(x)$, was calculated by inverse Fourier transform of $MTF_p(u)$. Assuming isotropic property, two dimensional $PSF_p(x,y)$ was obtained from $PSF_p(x)$.
2. Patch images whose dot coverage rate are 0.125, 0.250, 0.375, 0.500, 0.625, 0.750, 0.875 and 1.000 printed on glossy paper were printed by the inkjet printer.
3. Images $r(x,y)$ and $t(x,y)$ were obtained by capturing patch images using the microscope with each light source for reflection and transmission, respectively.
4. Paper images $r_p(x,y)$ and $t_p(x,y)$ were obtained using the microscope, respectively. Note that it is impossible to obtain $r(x,y)$ and $r_p(x,y)$ ($t(x,y)$ and $t_p(x,y)$) with same spatial region like the previous section since we cannot remove ink jetted on the paper. However, it is tiny problem since glossy paper has hardly fiber structure as shown in Fig. 6(b)(e).
5. Two images, $r_i(x,y)$ and $t_i(x,y)$, were obtained using Eqs. (12) and (13).
6. The transmittance distribution of ink, $t_i(x,y)$, was substituted into t_i of left-hand side of Eq. (22) for each x , and

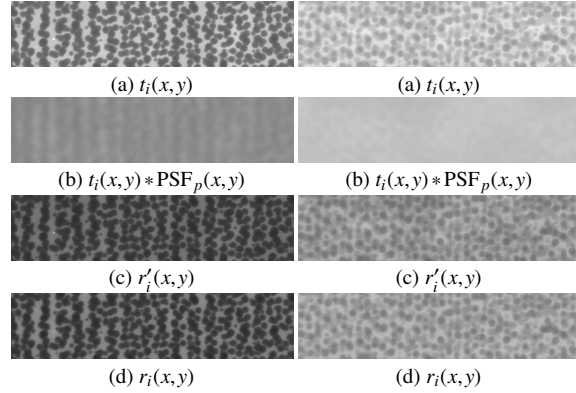


Figure 10. Dot coverage rate is **Figure 11.** Input pixel value is 512 0.250 (using unity type of ink). (using five types of ink).

Table 1. The RMSEs between $r'_i(x,y)$ and $r_i(x,y)$ (using unity type of ink).

Dot coverage rate	0.125	0.250	0.375	0.500	0.625
RMSE	0.049	0.037	0.014	0.011	0.0074
			0.750	0.875	1.000
			0.0080	0.0054	0.0051

Table 2. The RMSEs between $r'_i(x,y)$ and $r_i(x,y)$ (using five types of ink).

Input pixel value	512	1024	1536	2048	2560
RMSE	0.055	0.036	0.019	0.0092	0.0073
			3072	3584	4095
			0.0095	0.0073	0.0063

compensated $t_i(x,y)$ was calculated.

7. We predicted the reflectance distribution of ink, $r'_i(x,y)$, using $PSF_p(x,y)$ and $t_i(x,y)$ based on the reflection image model (Eq. (1)):

$$r'_i(x,y) = \{t_i(x,y) * PSF_p(x,y)\}t_i(x,y). \quad (25)$$

8. The root mean square error (RMSE) between the predicted $r'_i(x,y)$ and measured $r_i(x,y)$ was calculated to evaluate the prediction accuracy.
9. Difference of average reflectance of $r'_i(x,y)$ and $r_i(x,y)$ was also compared to evaluate the prediction accuracy.

Figures 10 and 11 show examples of the images obtained in this experiment. When five types of ink were used to print, we couldn't know the halftone algorithm of the printer. From this reason, we used input pixel value having 12bit dynamic range such as 512, 1024, 1536, 2048, 2560, 3072, 3584 and 4095 instead of dot coverage rate. Table 1 shows the results of RMSE for each dot coverage rate. Table 2 shows the results of RMSE for each input pixel value. Figure 12 shows the difference of average reflectance between the measured and predicted distribution for each dot coverage rate, respectively. Figure 13 shows the difference of average reflectance for each input pixel value, respectively. In these results, the reflectance distribution was approximately predicted with high accuracy since both the RMSE and difference of average reflectance are low. We consider some amount of error is

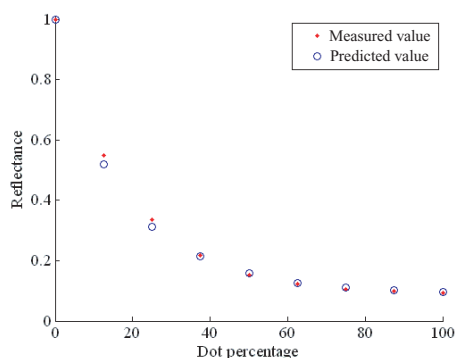


Figure 12. The average reflectance for each dot coverage rate (using unity type of ink).

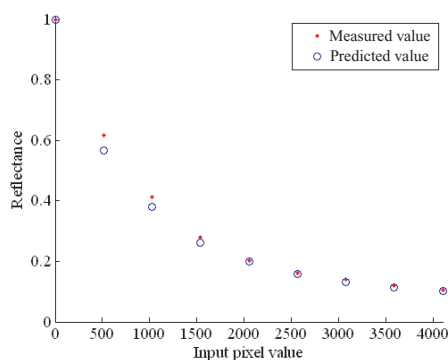


Figure 13. The average reflectance for each input pixel value (using five types of ink).

caused by 1) the fact we used Eq. (22) obtained by analyzing ND filter superposed on paper for compensating transmittance of real ink, 2) multiple reflections between the ink layer and paper layer and 3) ink penetration into paper.

This experimental result can be summarized that reflectance distribution of inkjet image can be predicted if we know transmittance distribution in case that paper has low graininess. Yamashita et al. propose a method for predicting transmittance distribution from input pixel value distribution [7]. If Yamashita's method and our method are combined, we can simulate inkjet printing process from input pixel value distribution to output reflectance distribution.

Conclusion

We modified the Koopipat's method for measuring the MTF of spatially non-uniform paper efficiently and accurately. First, we cancelled the fiber structure of paper causing noise of measured MTF by revising the reflectance and transmittance of paper from constant value to function of spatial coordinates in the reflection and transparency image models, respectively. Secondly, we introduced Gans' method for Fourier analysis of the ESF instead of derivation operation causing to amplify the noise.

Using the proposed method, three types of paper, uncoted, coated and glossy paper, were analyzed to measure the MTF, re-

spectively. Despite the high graininess of uncoated paper caused by the fiber structure, the measured MTF curve was much smooth and stable. The measured MTF curves of the coated and glossy paper were also smooth and stable. From this results, we consider our method is effective.

We predicted the reflectance distribution of monochrome inkjet images printed on the glossy paper from the transmittance distribution of that using the measured MTF of glossy paper based on the reflection and transparency image models. The accuracy of prediction was evaluated by the RMSE and difference of average reflectance between the measured and predicted data. These evaluations demonstrated the good prediction.

As future works, the same prediction experiment will be performed for the uncoated and coated paper. And we will perform the overall inkjet print simulation from the input pixel value distribution to the final reflectance distribution of printed image.

Acknowledgements

The authors wish to thank Mr. K. Suzuki, Mr. H. Sada and Mr. T. Ogura in CANON Inc. who provided the medical inkjet printer.

References

- [1] S. Inoue, N. Tsumura and Y. Miyake, Measuring MTF of Paper by Sinusoidal Test Pattern Projection, *Journal of Imaging Science and Technology*, vol.41, no.6, pp.657-661, Nov./Dec. (1997).
- [2] S. Inoue, S. Yamazaki, N. Tsumura and Y. Miyake, An Evaluation of Image Quality for Hardcopy Based on the MTF of Paper, *Journal of Imaging Science and Technology*, vol.44, no.3, pp.188-195, May/June (2000).
- [3] C. Koopipat, N. Tsumura, Y. Miyake and M. Fujino, Effect of Ink Spread and Optical Dot Gain on the MTF of Ink Jet Image, *Journal of Imaging Science and Technology*, vol.46, no.4, pp.321-325, (2002).
- [4] M. Ukishima, T. Nakaguchi, K. Kato, Y. Fukuchi, N. Tsumura, K. Matsumoto, N. Yanagawa, T. Ogura, T. Kikawa, Y. Miyake An Evaluation of Sharpness in Different Image Displays Used for Medical Imaging, *Proc. SPIE*, vol.6059-12, (2006).
- [5] A. S. Chawla, H. Roehrig, J. Fan and K. Gandhi, Real-time MTF evaluation of displays in the clinical arena, *Proc. SPIE*, vol.5029-84, Feb, (2003).
- [6] W. L. Gans and N. S. Nahman, Continuous and discrete Fourier transforms of step-like waveforms, *IEEE Trans. Instrum. Meas.*, IM-31, pp.97-101, June, (1982).
- [7] J. Yamashita, H. Sekine, T. Nakaguchi, N. Tsumura and Y. Miyake, Spectral based analysis and modeling of dot gain in ink-jet printing, *International Conference on Digital Printing Technologies IS&T's NIP19*, 769-772, (2003).

Author Biography

Masayuki Ukishima received the B.E. and M.E. degrees from Chiba University, Japan in 2005 and 2007. He is currently a doctoral course student in Chiba University, Japan. He is interested in image analysis and evaluation of image quality.